Effect of magnetic island on three-dimensional structure of edge radiation and its consequences for detachment in LHD (EX-D)

E.A. Drapiko 1), B.J. Peterson 1), M. Kobayashi 1), S. Masuzaki 1), T. Morisaki 1), M. Shoji 1), M. Tokitani 1), N. Tamura 1), S. Morita 1), M. Goto 1), S. Yoshimura 1), J. Miyazawa 1), N. Ashikawa 1), D.C. Seo 2), H. Yamada 1) and the LHD Team 1)

1) National Institute for Fusion Science, Toki 509-5292, Japan
2) National Fusion Research Institute, Daejeon 305-333, Rep. of Korea

E-mail contact of main author: drapiko.evgeny@lhd.nifs.ac.jp

Abstract. Detached plasmas represent an important operational regime for a fusion reactor whereby the heat load to the divertor can be reduced through enhanced radiation to ensure sustainable steady-state discharges. Normally, in toroidal devices there exists a density threshold above which detachment occurs, but in LHD the plasma commonly experiences radiative collapse before this threshold is reached. Recent work on LHD has shown the addition of an n/m=1/1 magnetic island (MI) enhances the detachment process by lowering its density threshold [1]. In this paper the effects of the MI on the 3D radiation structure in attached and detached plasmas as predictied by EMC3-EIRENE [2] are clearly seen in the imaging bolometer (IRVB) [3] data, experimentally confirming the role that the MI plays in the detachment process. With the addition of the MI the carbon radiation profile from the code in a poloidal cross-section becomes more localized near the helical divertor (HD) x-points (X). This is reflected in the focussing of the radiation patterns corresponding to the HDX in both the IRVB and code data in images corresponding to the IRVB field of view (FOV). Detachment results in a more asymmetric radiation profile in the poloidal cross-section code data with localized peaks near the HDX and MIX. The radiation from the MIX is reflected in strong radiation from the corresponding location in the IRVB FOV from both code and IRVB data. However the relative increase in the radiation from the MIX is greater in the code data than in the IRVB data for reasons which are so far unknown. Also similar discharges with and without the MI show detachment with the MI, albeit at a lower density than the discharge without the MI. This work confirms the previous conclusion that the MI enhances the localization of the radiation and is conducive to achieving and sustaining the detachment [1].

1. Introduction

Recent upgrade of the LHD IRVB [5] with a tangential field of view provides very informative 2D images of the radiation patterns from plasma. Combining experimental data with the synthetic diagnostic and EMC3-EIRENE [2] transport code results, obtained 2D images could be analyzed as a semi 3D. The result is a tool for the investigation of radiation behavior for 3D devices like LHD. It was shown that the addition of n/m=1/1 magnetic island has a stabilizing effect on the plasma detachment. The EMC3-EIRENE transport code was predicting a certain change in radiational pattern, namely the localization of the radiation near Helical Divertor X point and x-point of magnetic island with the detachment. Such localization provides a significant decrease of the diverter load. This pattern change was observed previously [1] experimentally with AXUV diodes data but the entire structure of the pattern and the influence of different plasma regions along the sightline of the detector was unknown. At the same time IRVB data gives very clear view of local radiation activity and there is a clear difference for the discharges with and without the island in good agreement with transport code results. In this paper we will try to show this agreement and try do give a more detailed description of the 3D geometry of the radiation spots accompanying plasma detachment.

2. Experiment setup

LHD has an unique coils system, along with regular helical and vertical field coils there are 20 saddle perturbation field coils which allows to add n/m=1/1 magnetic island to the steady state configuration. For the experiments described in this report the vacuum magnetic axis is located at a major radius of 3.9 m and the average minor radius is ~ 70 cm. Plasma heating was accomplished by 3 tangential negative ion based neutral beams (NB) with a nominal acceleration voltage of 180 keV.

The InfraRed imaging Video Bolometer (IRVB) [5] used in this study has a tangential field of view of the plasma as shown in Fig. 2. The number of channels (bolometer pixels) is 16 horizontal and 12 vertical and the frame rate is 237 frames per second. Direct comparison of the transport code results and IRVB data is unclear because its measurements are integrated along the detector sightline and the calculation is a 3D array of carbon radiation. Thus to make a comparison we have developed a synthetic dignostic which provides a simulated IRVB image calculated from EMC3-EIRINE code results, taking into account the geometry, pinhole position, field of view, obstacles (walls, constuction elements etc) resulting in the socalled geometry matrix. This matrix being multiplied by the 3D matrix of data of carbon radiation will give us the resulting image for IRVB the [6]. Moreover, the code uses a different coordinate system and very fine grid which absolutely unneccesery for this particular case. So we have been also resampling the data to the cylindrical grid with 5 cm steps in major radius R, and vertical dimention Z and a 1 degree step for toroidal angle ϕ. Also, the IRVB raw image has to be preproccesed taking in to the account the calibration data (local thermal characteristics of the IRVB foil), by solving the heat diffusion equation for a given heat distribution and IR camera calibration data.

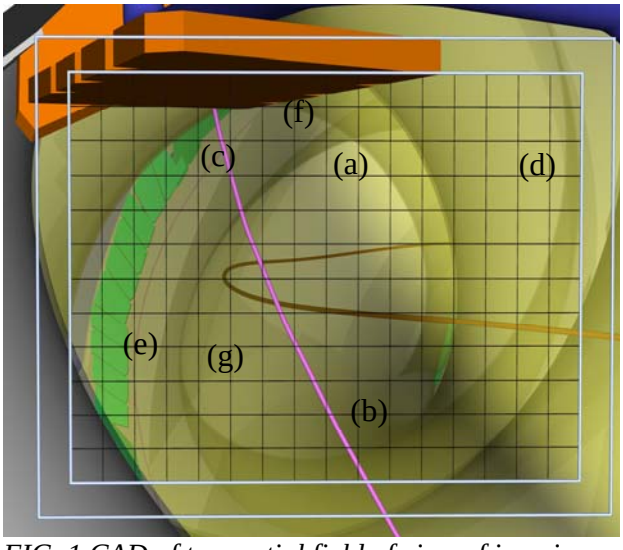

FIG. 1 CAD of tangential field of view of imaging bolometer on LHD.

3. Discharge parameters with and without a MI

For this paper we will consider two similar discharges, LHD#97365 and LHD#97327 the only difference is the absence and presence of the magnetic island and slightly higher density without island. Figure 3 shows waveforms for some plasma parameters with detached ones dashed. For both cases one of the NBs is terminated 0.7 to 0.9 seconds prior to the termination of the other NBs reducing the absorbed power by about a factor of two as can be seen in the thick lines in Fig. 3 (a). The plasma with the MI applied detaches from the diverter as one could see from several diagnostics data shown. Namely, the increase in the carbon IV signal (2s-2p transition at 1549 Angstroms) by the factor of 5 for MI case, total radiated power increase 3(d), the ion saturation currents from the divertor probe signals in Fig. 3 (f) indicate detachment in the case of the MI as the reduction in the signals is greater in the case of the MI at both at top and upper location, the H_γ/H_β ratio step, showing the volume recombination processes associated with the detachment. In the case without the MI the plasma does not detach even though it reaches a higher density as can be seen in Fig. 3 (c). This confirms the conclusions of the previous work [2] that show that the MI can help to induce and stabilize divertor detachment.

4. Effect of MI on location of radiation and detachment

At first we will try to compare 2D images of code results and measurements in order to determine the effect of the MI. There are three plasma cases shown from the two discharges in Figs.3-5. Namely (a) attached without MI and at low density, (b) attached with MI at the same low density as (a) and (c) at higher density with MI and detachment. Fig. 4 shows the impurity radiation intensity from carbon in the edge region at the vertically elongated cross-section of LHD from the code [2]. Fig. 5 shows the same code data integrated into the tangential field of view (FOV) of the IRVB using the synthetic instrument. Fig. 6 shows the corresponding 12 x 16 channel IRVB radiation data. Pink lines show the traces of the HDX, thicker line corresponds to the nearer field. Fig. 4(a) shows fairly poloidally uniform pattern while the addition of the MI results in more localized peaks near the HDX and MIX (red circle). We can almost clearly observe such a pattern change at Figs 5 and 6. After adding the MI, the pattern, as shown at Fig. 5(b), changes to a clear trace of the HDX, so do the measurements result at Fig. 6(b). Detachment gives an even more localized and asymmetric radiation peaks at MIX Fig. 4(c). This should result, as code predicted, very intense radiation peak at MIX Fig. 5(c) which brighter than the HDX pattern. Measurement results at Fig. 6(c) show only a slightly increase of the radiation peak at the MIX and even more localized pattern in general.

In order to observe the pattern behavior in time lets consider a small number of spots on the 2D image. Fig. 7 shows those 7 spots of interest. The detached case with MI is shown with a dashed line. The (a) spot is some far field spot which start shining by the end of the discharge indicating the radiative decay, (b) presumable spot of MIX location, (c) the most intense spot corresponding to the crossing point of far and near HDX traces, (d) gives us some information of radiation from the HDX at the top inboard part, which is barely seen by the IRVB, (e) far field HDX, (f) spot right above the divertor plates at near field, (g) some spot from the core. Fig. 8 shows the time trends of the radiated power for above mentioned spots. Thus, waveforms a – d show large increases with the detachment and decay events, while the other three (e, f, g) do not. The MIX spot gives the highest radiated power increment among others, from 0.020 to 0.035 mW, while the most intense spot (c) gives increment is from 0.025 to 0.035 mW. The spot (a) which gives clear radiative decay indication as a spike at 6.1

s. for the attached case does not show the same pattern for the detached one. The core radiation as one could see from Fig 7(g) seems not to be involved in the detachment process at all, so the assumption for the EMC3-EIRENE transport code taking into the account only edge regions of plasma seems to be reasonable. There is a difference in the time behavior for the near and far HDX traces, which could be seen at Fig. 7(c,e). Thus the far HDX trace gives lower radiation power for the detached case, while the near HDX dominates the radiation for the detached plasma. The divertor spot signal also does not show any connection to the detachment Fig. 7(f).

5. Conclusion and discussion

This paper is the first example of the detached plasmas in LHD observed by IRVB. Measurements results along with the synthetic diagnostic applied to the EMC3-EIRENE transport code show good agreement. Comparing the modeling results with the measurements we can state that even raw 2D images from the IRVB could be very informative and usefull for analysis of the radiation phenomena especially for 3D devices like LHD. Experimental results confirm the assumption of the basic role of edge plasmas and carbon as the main impurity for this type of discharges. IRVB images show that addition of the MI localize the radiation at HDX and encreases the radiation from the MIX as was predicted by the code. The discharge termination after all NBI stopped is more smooth for the detached case. Also, the divertor plates region placed within the FOV of IRVB does not show any connection to the detachment according to the radiated power signal. This could be because of the very high radiation peak from the near and far HDX crossing in the vicinity. Difference in the behavior of the radiation paterns for the near and far HDX traces could be explained by the toroidal asymmetry in the radiation pattern due to the MI.

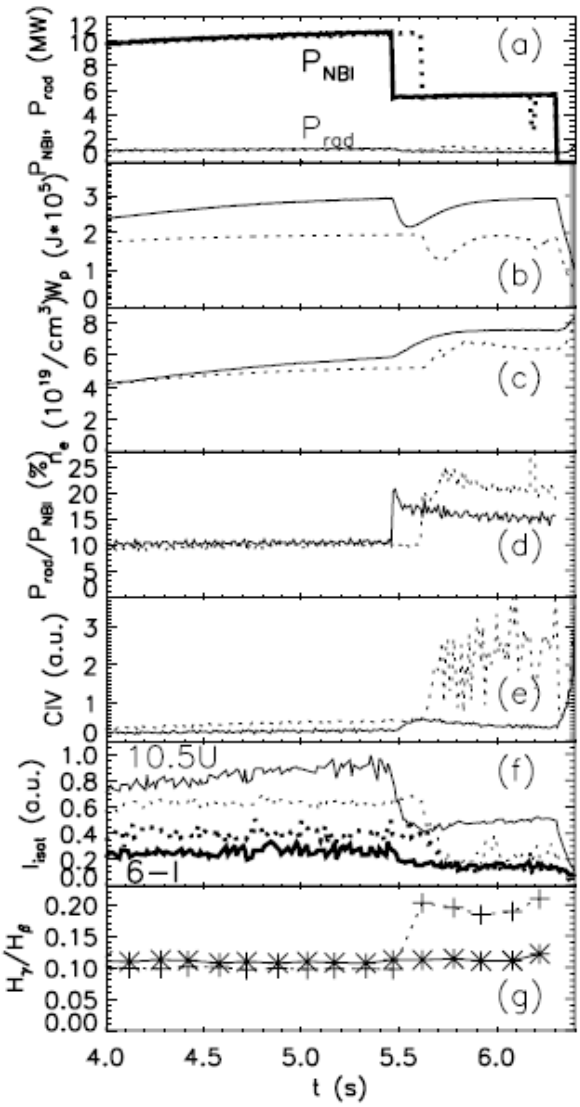

FIG. 3 Temporal evolutions of (a) NB absorbed power (thick) and radiated power (thin), (b) stored energy, (c) electron density, (d) radiated power fraction, (e) carbon IV, (f) divertor ion saturation current at upper port (thin) and inboard port (thick) for shots with MI (dashed) and without MI (solid), (g) H_γ/H_β ratio for shots with MI (dashed) and without MI (solid).

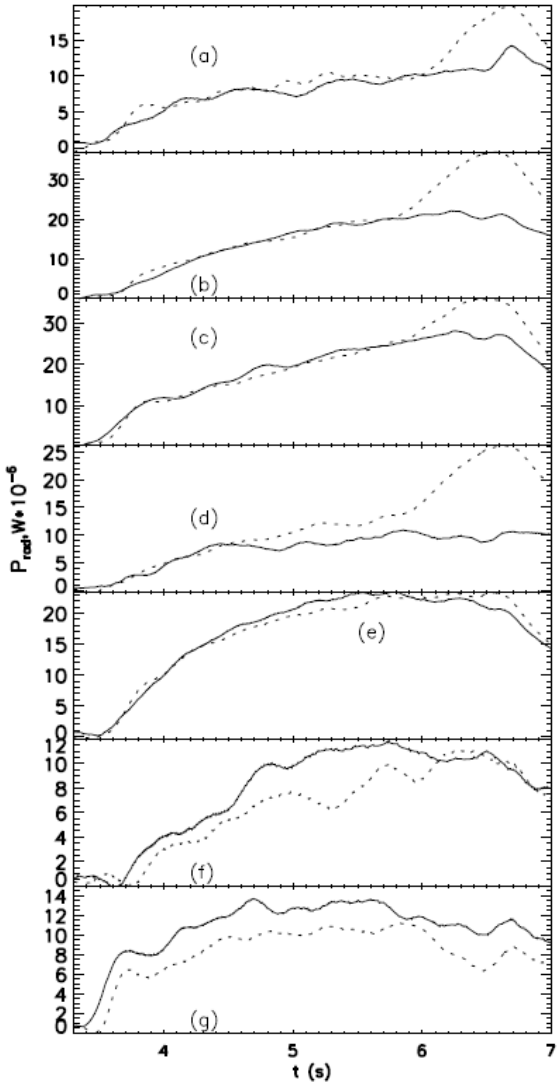

FIG .8 Time traces of different spots (a) far field spot with good indication of the radiative collapse, (b) spot of approximate MIX location, (c) crossing spot for near and far HDX traces, (d) inboard top spot, (e) far field HDX trace, (f) spot right above the divertor plate, (g) core spot

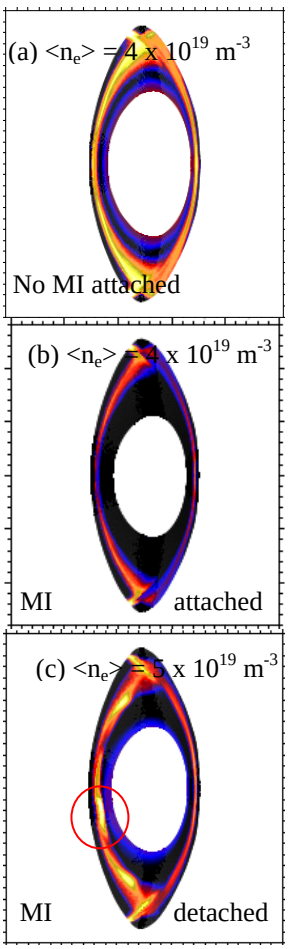

Fig. 4 Radiated power from model [2] for attached plasmas at LCFS n_e of 4 x 10^{19} m^{-3} (a) without and (b) with MI, and (c) detached plasma with MI at 5.5 x 10^{19} m^{-3} LCFS n_e.

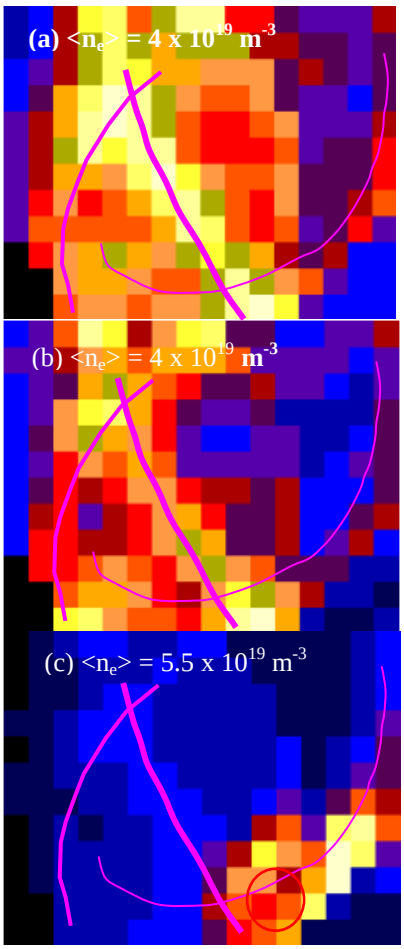

Fig. 5 Model [2] results shown in Fig. 4 line-integrated into IRVB field of view. With addition of MI in (b) radiation pattern becomes more focused. Red circle indicates localized region of radiation from MI x-point during detachment in (c).

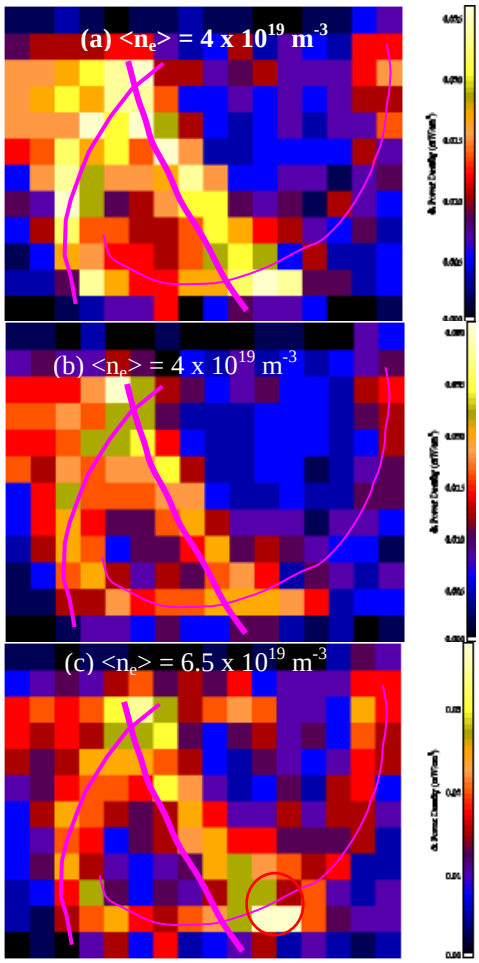

Fig.6 IRVB data showing radiation from plasmas attached (a) without and (b) with MI and (c) detached plasmas with an MI. Red circle shows localized region of radiation from MI x-point corresponding to that shown in Figures 3(c) and 4(c).

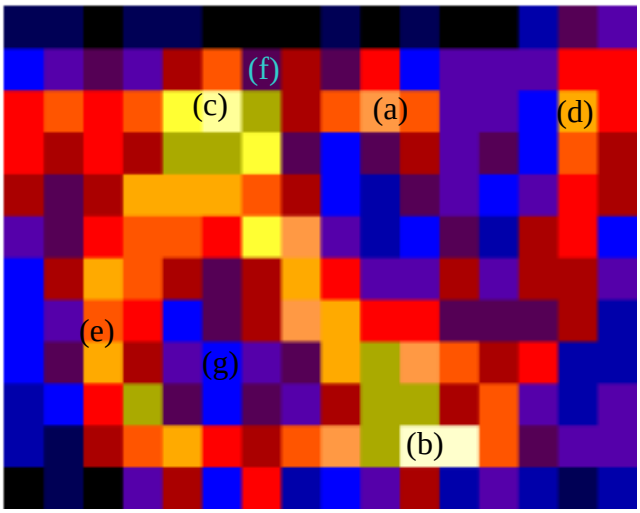

Fig. 8 Spots for time traces

Appendix 1: References

[1] G. F. Matthews, J. Nucl. Mater. **220-222** 104 (1995).

[2] M. Kobayashi et al., Phys. Plasmas **17**, 056111 (2010).

[3] Y. Feng et al., Contrib. Plasma Phys. **44**, 57 (2004).

[4] D. Reiter eta al., Fusion Sci. Technol. **47**, 172 (2005).

[5] B. J. Peterson et al., to be published in Plasma Fusion Res. (2010).

[6] B.J. Petersona et al., submited to Nuclear Materials.